

Analysis of Spatiotemporal Patterns in a Model of Olfaction

Orit Kliper ^{a,1} David Horn ^b Brigitte Quenet ^c Gideon Dror ^d

^a*School of Mathematical Sciences Tel Aviv University Tel Aviv, 69978, Israel*

^b*School of Physics and Astronomy Tel Aviv University Tel Aviv, 69978, Israel*

^c*Lab. d'Electronique, Ecole Supérieure de Physique et Chimie Industrielles, Paris 75005, France*

^d*Department of Computer Science, The Academic College of Tel-Aviv-Yaffo, Tel Aviv 64044, Israel*

Abstract

We model spatiotemporal patterns in locust olfaction with the Dynamic Neural Filter (DNF), a recurrent network that produces spatiotemporal sequences in reaction to sets of constant inputs. We specify, within the model, inputs corresponding to different odors and different concentrations of the same odor. Then we proceed to analyze the resulting spatiotemporal patterns of the neurons of our model. Using SVD we investigate three kinds of data: spatiotemporal patterns over the period of odor presentation, total spike counts during this period, and spatial information of single temporal bins.

Key words: Olfaction; Temporal Coding; Dynamic Neural Filter; Recurrent Network

1 Introduction

The Dynamic Neural Filter (DNF) (2) is a recurrent binary neural network that maps regions of input space into spatiotemporal sequences. It has been motivated by locust olfaction research. Here we take up the task of using this model as a prototype of spatiotemporal patterns, and put it to tests of the kind employed by (1) for data obtained from the locust antennal lobe.

¹ Corresponding author. e-mail: klipor@post.tau.ac.il

Since this kind of system is known to exhibit a local field potential with temporal width of 50ms (6), we take this time window as the basic temporal bin in our discrete system, obeying

$$n_i(t+1) = H(h_i(t+1)) = H(\sum_j w_{ij}n_j(t) + R_i - \theta_i) \quad (1)$$

where n_i are the neural activity values, w_{ij} is the synaptic coupling matrix, R_i is an external input and θ_i is the threshold. H is the Heaviside step function taking the values 0 for negative arguments and 1 for positive ones. For simplicity we choose w_{ij} as integers, fixing $\theta_i = \frac{1}{2}$. The initial (background) state will have random low activity.

In the next section we define all other details of the model, after which we turn to a series of numerical experiments and their analysis.

2 Model of Olfaction

We use a fully connected binary network, defined by an asymmetric weight-matrix, with $tr(\mathbf{w} \cdot \mathbf{w})/tr(\mathbf{w} \cdot \mathbf{w}^T) \approx 0$, having both positive and negative couplings taken from a normal distribution of width 5. In a previous work (3) we discussed some features of the response sequences generated in large networks e.g. $N = 40$, by changing R values. We found that close-by R values generate divergent spatio-temporal sequences. We also found that the center of R space is the region where the system leads to large cycles and chaotic-like phenomena of total divergence occur. As we move out of the center of this space, small changes in R may lead to divergence, but finite correlations survive. These findings were consistent with the experimental results (4) in the olfactory bulb of zebrafish. Fix points and short cycles appear mostly at the edges of the relevant R space, as defined in (2), and are not relevant to the current olfaction model.

Let us limit ourselves to an 'active range' of R space where almost all sequences are long. This range can be defined by the standard deviation of the distribution of h , over all neurons and all time steps, in response to input at the center of R space. Numerical simulations lead to active ranges of 5 for $N=5$, 13 for $N=25$ and 18 for $N=50$.

Turning to olfaction, we note that (5) have demonstrated a logarithmic relationship between the inputs (odors) at different concentrations and the receptors' response. Making use of this result, we map five orders of odor concentration onto the 'active range' of R . An odor is represented by a ray in input space, and different concentrations are identified by different locations on the

odor's ray. The starting points of all rays (odors) are mapped to a region close to the lowest corner of the 'active range'. Noise is added to the resulting R values to represent stochastic fluctuations.

This model is supposed to represent the antennal lobe of locust. Although no attempt was made to distinguish between excitatory and inhibitory cells, or to follow other anatomical and physiological elements of the biological system, it may serve as a rudimentary model of the spatiotemporal behavior observed in this system. In particular, it allows us to investigate some interesting questions following from the analysis of such systems, comparing results of our model with those revealed in experiments (1).

3 Analysis of the spatiotemporal data

Similar to the work of (1) the data we analyzed were spatiotemporal patterns of randomly selected 15 neurons over the whole simulation time. Figure 1 depicts such patterns, derived from a network of 100 neurons, 75 of which received a constant odor during 60 time steps. Each of the three frames, representing three concentrations of the same odor, will be referred to as a 'spatiotemporal pattern'. We proceed then to ask for clustering properties of such patterns for different odors and different concentrations.

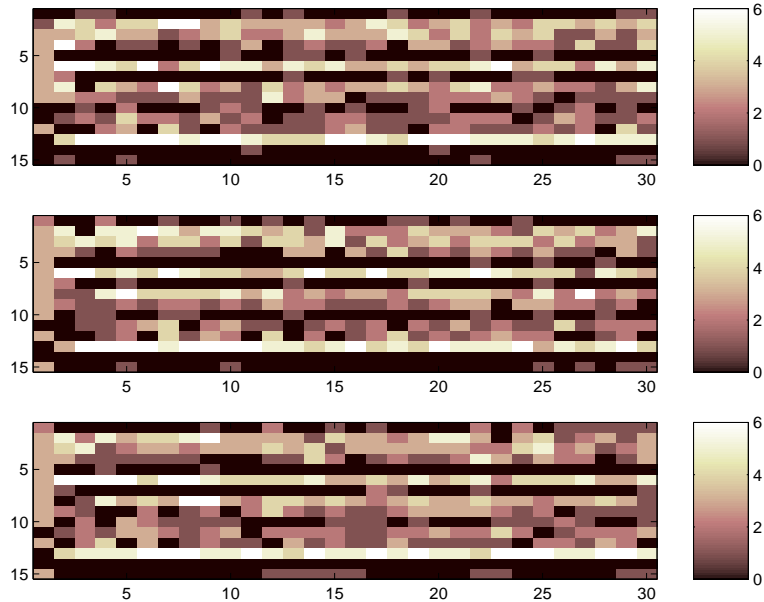


Fig. 1: Spike counts for three different concentrations of one odor summed over three trials. The 60 time steps are binned into 30 bins of 100ms each.

3.1 Singular Value Decomposition

We choose SVD as our tool for dimensionality reduction. It is applied to the set of all data. For each odor and concentration we generate 5 data points, each representing an average over 3 trials (differing from one another by noise). Thus we have 75 data (25 for each odor, 5 for each concentration) each having a 450 dimensional spatiotemporal pattern. SVD is applied to this 75×450 matrix, truncating it down to 3 dimensions (corresponding to the three, or three out of the four, leading variance-eigenvalues), and projecting onto two dimensions. The 75 points may now be represented on these three dimensions. In our representation we take care of normalizing these points to a common norm 1. An example is presented at figure 2. Clusters of both odor and concentration exist. Thus we conclude that the spatiotemporal patterns include this information, and it can be easily retrieved via SVD.

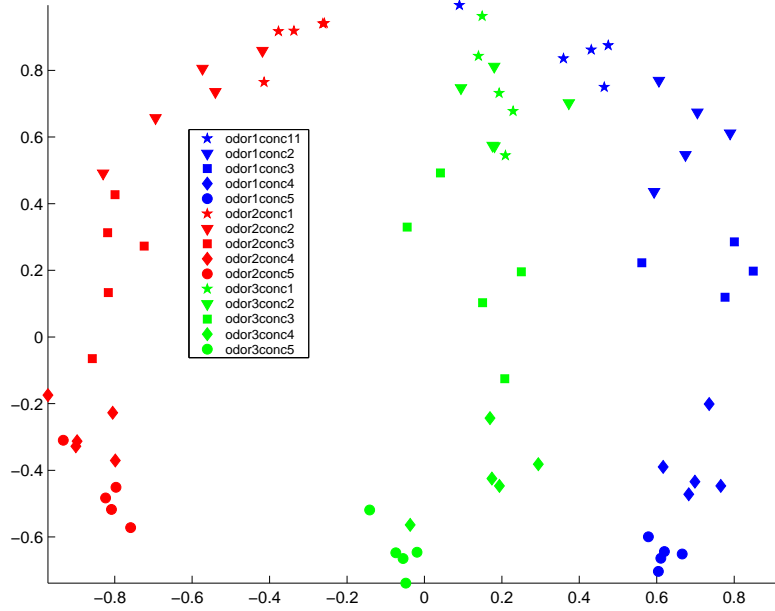


Fig. 2: A 2-dimensional projection of the SVD representation of the spatiotemporal patterns. Different colors represent different odors, while shapes represent concentrations. Clear clusters by odor and by concentration appear.

Next we ask ourselves if that type of information exists already at the level of single temporal bins, i.e. the columns of the spatiotemporal patterns discussed above. To answer this question we apply SVD to a matrix of 2250×15 , corresponding to 75×30 data-points (including the specific temporal bins) and 15 neural spatial patterns. The results, shown in Fig. 3 reveal clustering of odors. For any individual odor, one can also obtain clustering of concentrations (not shown here).

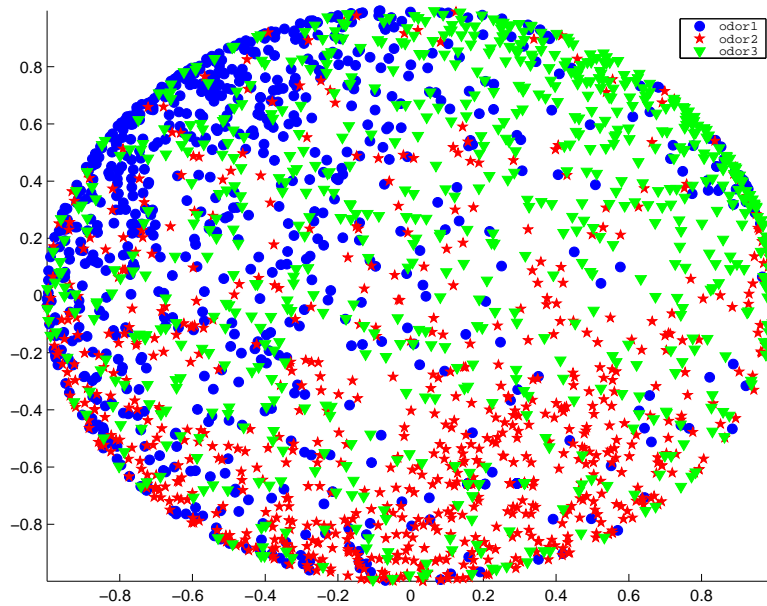


Fig. 3: 2-dimensional projection of the SVD reduction of spatial data for individual temporal bins. Data comprised 2250 points, represented here by 3 colors specifying the three odors.

Our third SVD experiment is to analyze the spike count data, i.e. we take the 75×450 matrix of data described above, and sum all columns (temporal-bins) together into 15 dimensional vectors, thus leading to a 75×15 data matrix. The resulting clustering properties were similar in quality to those of Fig. 2. Hence we conclude that the responses to different odors and different concentrations can be distinguished by the total spike counts, i.e. the information is carried by a rate code.

All these simulations were carried out under the assumption that the system is subjected to a constant odor throughout the numerical experiment. To check ourselves with respect to the experimental results of (1) we proceeded to define a second set of numerical experiments, where a constant odor (with small noise) was turned on for 1 sec, followed by 2 sec of no odor (background activity). The results are that the spatiotemporal patterns (the 75×450 matrix) retain the power to cluster different odors and concentrations, but this does no longer hold for either the column analysis (the 2250×15 matrix) or the spike count (rate coding).

4 Discussion

Although the last conclusion favors spatiotemporal coding, it is disappointing that the column analysis did not lead to meaningful results. In particular, the

temporal columns did not form any particular order within the clusters. This does not agree with (1), who have demonstrated that column analysis leads to an interesting representation of different odors lying on different manifold and different concentrations corresponding to different trajectories on these manifolds. We suspect that the reason our model did not lead to the same result is that the DNF, with its one time-step dynamics, lacks some sort of short term memory, that carries the odor information after it is being removed. We are in the process of investigating synaptic dynamics, searching for the correct paradigm that will lead to meaningful temporal coding.

References

- [1] Stopfer M., Jayaraman V. and Laurent G. Spatiotemporal codes for odor identity and concentration (submitted) (2003).
- [2] B. Quenet and D. Horn, 2002. The Dynamic Neural Filter: A Binary Model of Spatiotemporal Coding. *Neural Computation* 15, in print.
- [3] D. Horn, B. Quenet, G. Dror, O. Kliper, 2002. Modeling Neural Spatiotemporal Behavior. *proceedings of CNS02*
- [4] R. W. Friedrich and G. Laurent, 2001. Dynamic optimization of odor representations by slow temporal patterning of mitral cell activity. *Science* 291, 889-894.
- [5] J.P. Rospars, P. Lansky, P. Duchamp-Viret, A. Duchamp, 2000. Spiking frequency versus odorant concentration in olfactory receptor neurons. *BioSystems* 58, 133-141
- [6] M. Wehr and G. Laurent, 1996. Odour encoding by temporal sequences of firing in oscillating neural assemblies. *Nature* 384, 162-166.